Validity of the effective-mass approximation for shallow impurity states in narrow superlattices

C. Priester, G. Allan and M. Lannoo

Laboratoire de Physique des Solides (Laboratoire associé No. 253 au Centre National de la Recherche Scientifique),
Institut Supérieur d'Electronique du Nord, 3 rue François Baës, F-59046 Lille Cedex, France
(Received 8 April 1983)

The applicability of effective-mass theory to the calculation of impurity binding energies is discussed. A numerical test calculation is first performed in the case of one single band. A new two-dimensional effective-mass approximation is then proposed, valid for a small and a moderately small (up to 15) number of planes, allowing determination of impurity states derived from any subband. It is then shown that Bastard's model yields accurate binding energies for the lower states where it is applicable. Finally tunneling effects between quantum wells are considered showing that they have a nonnegligible influence in the experimental conditions.

I. INTRODUCTION

Since the development of molecular-beam epitaxy, there has been great interest in semiconductor superlattices, first realized by Esaki and Tsu.[1,2] Many absorption and luminescence experiments have been performed[3-7] and excitons have been observed. A simple and analytical theory of these systems has been proposed by Bastard[8] using a three-dimensional effective-mass approximation [3D EMA (refined treatment has been proposed recently in Ref. 9)]. This theory is based on the following assumptions: (i) the discontinuities in potential are assumed to be large so that the study is limited to an isolated quantum well, (ii) the quantum well is simulated by an infinite square well, the effective kinetic energy operator being obtained from the 3D EMA, and (iii) the impurity potential is superposed to the constant potential in the quantum well.

It is clear that such a treatment is valid for a large number of planes in the quantum well. It should become inadequate[10] in the limit of a few planes since the potential does no more fulfill the criterion of being slowly varying.[11] However, it is important to know at which stage these approximations become poor and what is the magnitude of the corresponding error. The present work tries to answer such questions. For this an "exact" test calculation is first performed for small number of planes in a simple case of a tight-binding s band with a Coulombic impurity. We also present a two-dimensional (2D) EMA which is tractable only for very narrow superlattices and compare it to the exact results. We then present a more useful 2D treatment which proves to be valid in the intermediate case, i.e., for a number of planes ranging from 1 to about 15. This treatment represents in fact the central result of this paper since it allows calculation of the binding energy with respect to the exact energy of the bottom of the corresponding subband, which is not the case in Bastard's model. Finally we discuss the validity of EMA for that problem and show that our 2D treatment provides the natural approximation method for moderately narrow and narrow superlattices.

II. EXACT CALCULATION FOR VERY NARROW SUPERLATTICES

Here we want to perform an exact numerical test calculation. For this we consider a single band with one Wannier function per atom. This is completely equivalent to a tight-binding s band. To get the maximum simplicity we consider only hopping integrals between nearest neighbors. The dispersion law for a perfect square lattice (corresponding to the limiting case of one plane) is then given by

$$E(\vec{k}_{||}) = -2\beta[\cos(k_x a) + \cos(k_y a)] , \qquad (1)$$

where β is the hopping integral and $\vec{k}_{||}$ is the wave vector within the plane of components k_x and k_y, a being the lattice parameter. The minimum in energy corresponds to $\vec{k}_{||}^{0} = 0$ and the effective mass near this minimum is given by

$$m^* = \frac{\hbar^2}{2\beta a^2} . \qquad (2)$$

We consider a donor impurity with attractive potential $V(\vec{r})$ assumed diagonal in the Wannier functions' basis.

Its value on the impurity site (taken as the origin of coordinates) is taken equal to U, while $V(\vec{R}_i)$, on site $\vec{R}_i \neq 0$, is given by

$$V(\vec{R}_i) = -\frac{e^2}{K |\vec{R}_i|} . \qquad (3)$$

This 2D impurity problem cannot be solved analytically. We have thus used a numerical technique based on Green's-function theory.[12] For this we calculate suitable diagonal matrix elements of the Green's operator by the continued-fraction—expansion technique.[13] The impurity states thus appear as poles of these Green's functions. Table I [part (a)] gives the results obtained for

$$U = -8, \quad \beta = 0.1, \quad a = 5, \quad K = 10 \qquad (4)$$

(with values for U, β, and a in a.u.), which correspond to

TABLE I. Values of $(E - E_0)$ in atomic units obtained using a numerical calculation (LCAO method on an s cubic lattice using a recursion method) and using the 2D EMA. (a) System made by one plane, and (b) system made by three planes (antisymmetrical solutions).

State	(a) One plane Exact calculation-2D EMA	(b) Three planes Exact calculation-2D EMA
E_{1s}	0.004 19-0.004 0	0.002 59-0.002 49
E_{2p}	0.000 441-0.000 444	0.000 434-0.000 417
E_{2s}	0.000 448-0.000 444	0.000 372-0.000 379

$m^* = 0.2m_e$, where m_e is the electron mass.

This method can be extended to the case of several planes, provided their number N remains small (in practice $N \leq 5$). For odd number of planes and a central impurity, the Coulombic potential is an even function of z (the coordinate normal to the planes) and we can separate even and odd solutions. Then we obtain even bound states under the even bands and odd bound states under the odd bands. These results are reported on Fig. 1 for $N = 1$, 3, and 5, and the two lower bands for which there exist true bound states. Let us notice that the lower "s" state under the odd band has rather the behavior of a "p_z" state which will asymptotically tend towards the impurity p state for a large number of planes.

III. 2D EMA FOR VERY NARROW SUPERLATTICES

The case of one plane with a central impurity can be handled by the usual techniques of effective-mass theory,[14-18] leading to the 2D effective-mass equation

$$\left[-\frac{\hbar^2}{2} \left[\frac{1}{m_x^*} \frac{\partial^2}{\partial x^2} + \frac{1}{m_y^*} \frac{\partial^2}{\partial y^2} \right] - \frac{e^2}{K |\vec{r}|} \right] f(\vec{r})$$
$$= (E - E_0) f(\vec{r}) , \quad (5)$$

where $f(\vec{r})$ is the envelope function. In our case $m_x^* = m_y^* = m^*$ given by (2), leading to an isotropic situa-

tion. Equation (5) can be solved using a polynomial method[19,20] and the energy eigenvalues are given by

$$E_{m,n} = -\frac{2m^* e^4}{K^2 \hbar^2} \left[\frac{1}{2(n+m)+1} \right]^2 . \quad (6)$$

The lower-energy levels obtained by this expression are compared in Table I [part (a)] to the exact values of Sec. II. The agreement is very good showing the quality of the predictions of EMA. However, we must notice that the numerical value of the 1s lower level is sensitive to U, i.e., to the chemical shift, and that the agreement obtained for that level is somewhat fortuitous. This is not true for excited states which are much less sensitive to U. To show this more clearly we have investigated the much less favorable (and unrealistic) case corresponding to $K = 1$ whose results are reported on Table II. While the agreement is much worse for the 1s state, it remains quite satisfactory for all other states, thereby demonstrating the power of the EMA.

When the layer contains a few planes (N), we can still use the EMA in directions parallel to the layer, but not perpendicular. In such a case it can be proven[21] that, instead of obtaining one single differential equation, we have to handle a system of N coupled differential equations which is extremely difficult to solve. However, for a system of three planes, it is still possible to obtain simple analytical results for the case of a central impurity for which we get a symmetrical system.

Let us then note as $|i,l\rangle$ the Wannier function centered on atom l of the ith plane, with $i = 1-3$. It is useful to build combinations of these atomic functions having well-defined symmetry properties. With the three functions $|1,l\rangle$, $|2,l\rangle$, and $|3,l\rangle$ we can build one antisymmetrical combination

$$|a,l\rangle = \frac{1}{\sqrt{2}} (|1,l\rangle - |3,l\rangle) \quad (7)$$

and two other symmetrical combinations. Thus, the antisymmetrical impurity states can be expressed in terms of the $|a,l\rangle$ alone which exactly reduces the problem to a 2D one. The only difference with the one-plane case comes from the matrix elements of the impurity potential. These are now given by

$$\langle a,l | V | a,l' \rangle = \frac{1}{2} [\langle 1,l | V | 1,l \rangle + \langle 3,l | V | 3,l \rangle] \delta_{ll'} ,$$
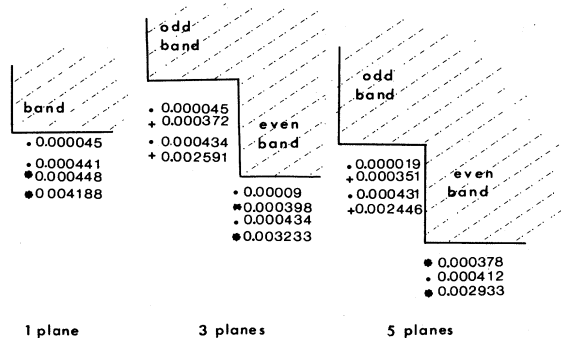$$(8)$$

i.e.,

FIG. 1. Even and odd bound states under the bands for a central impurity in a system made by 1, 3, or 5 planes calculated by LCAO. An asterisk indicates an s state bound to the chemical shift, a dot indicates a p state, and a plus sign indicates an s state unconnected to the chemical shift. The numbers are the distance to the bottom of the band in atomic units.

TABLE II. Localized states under the bottom of the band; for a donor impurity in a single plane: Distance between the state and the bottom of the band, $K = 1$, is (a) calculated using a LCAO method with $\beta = 0.1$ a.u. and $a = 5$ a.u., and calculated (b) using the EMA.

State	(a)	(b)
$1s^a$	2.631	4.00
$2s^a$	0.474	0.444
$2p$	0.451	0.444
$3s^a$	0.172	0.160
$3p$	0.164	0.160
$4s^a$	0.085	0.082
$4p$	0.083	0.082
$5s^a$	0.052	0.049
$5p$	0.050	0.049
$6s^a$	0.034	0.031
$6p$	0.033	0.031

[a]These states are bound to the chemical shift.

$$\langle a,l \mid V \mid a,l' \rangle = -\frac{e^2}{K(R_l^2 + a^2)^{1/2}} \delta_{ll'} , \qquad (9)$$

instead of $-e^2/KR_l$ for one plane. We have then simply to solve Eq. (5) but where the potential is replaced by $-e^2/K(r^2 + a^2)^{1/2}$.

The solution of this new problem cannot be found exactly and we use a variational procedure. For the lower "$1s$" state we take a trial function

$$f_{1s}(r) = Ae^{-\alpha r} . \qquad (10)$$

The expectation value of the EMA Hamiltonian in this case can be expressed under the form

$$E_{1s}(\alpha) = \frac{\hbar^2}{2m^*}\alpha^2 + \frac{4e^2\alpha^2 a}{K}\{1 - (\pi/2)[H_1(2\alpha a)$$
$$- N_1(2\alpha a)]\} , \qquad (11)$$

where H_1 and N_1 are the Struve and Neumann functions of order 1.[22] The function $E_{1s}(\alpha)$ is then minimized numerically leading to optimal values α_m and $E_{1s}(\alpha_m)$.

A similar procedure can be rigorously applied to the "$2p$" state which, by symmetry, is automatically orthogonal to the $1s$ state. In that case we take a trial function of the form

$$f_{2p}(r,\theta) = Are^{-\alpha r}\cos\theta , \qquad (12)$$

and can express the quantity $E_{2p}(\alpha)$ in terms of Struve and Neumann functions of order 0 and 1, and then minimizing with respect to α.

The case of the "$2s$" state cannot be handled rigorously from the variational point of view since we cannot orthogonalize it to the exact $1s$ state. We have, however, chosen for this state a trial function

$$f_{2s}(r) = A(b - r)e^{-\alpha r} , \qquad (13)$$

where b is determined by orthogonalization to the approximate $1s$ state obtained above. From this we can then determine $E_{2s}(\alpha)$ and minimize it, the procedure, at this point, having an indicative value.

The corresponding results are reported in Table I [part (b)] showing very good agreement with the results obtained from the exact numerical calculation. This again shows the usefulness of the 2D EMA for that problem.

IV. MORE GENERAL 2D EMA

The treatment developed just before is a discrete method that can treat only very few planes ($N \leq 3$). For instance, the case $N = 5$ with a centered impurity cannot be decoupled since there are two symmetric coupled equations and three antisymmetric coupled equations. It is thus of considerable interest to devise a more general method to reduce the problem to a 2D effective-mass equation. We shall adapt for this the general method which allows us to derive the 3D EMA in $\vec{k}$ space.

Let us then denote as H_0 the Hamiltonian of the superlattice in the absence of the impurity. Its eigenvalues can be grouped into 2D subbands which result from quantification in the z direction. For small N the distance in energy between the bottoms of these different subbands are much larger than the binding energy of the impurity states. We can thus say that in this limit each set of impurity states derives from the corresponding 2D subband (we neglect here resonance effects which are discussed in a forthcoming paper[23]). We thus write the impurity states $| \Psi_n \rangle$ derived from the nth 2D subband under the form

$$| \Psi_n \rangle = \sum_{\vec{k}_{\parallel}} a_{n,\vec{k}_{\parallel}} | \varphi_{n,\vec{k}_{\parallel}} \rangle , \qquad (14)$$

where $| \varphi_{n,\vec{k}_{\parallel}} \rangle$ are the Bloch states relative to this subband. Projecting the Schrödinger equation onto one of the basis states $| \varphi_{n,\vec{k}_{\parallel}} \rangle$ we get

$$[\epsilon_n(\vec{k}_{\parallel}) - E]a_{n,k_{\parallel}} + \sum_{\vec{k}_{\parallel}'} \langle \varphi_{n,k_{\parallel}} \mid V \mid \varphi_{n,k_{\parallel}'} \rangle a_{n,\vec{k}_{\parallel}'} = 0 , \qquad (15)$$

where $\epsilon_n(\vec{k}_{\parallel})$ is the dispersion relation for the nth subband and V is the impurity potential. Writing $| \varphi_{n,\vec{k}_{\parallel}} \rangle$ under the Bloch form we get

$$\langle \varphi_{n,\vec{k}_{\parallel}} \mid V \mid \varphi_{n,\vec{k}_{\parallel}'} \rangle = \int e^{i(\vec{k}_{\parallel}' - \vec{k}_{\parallel})\cdot\vec{r}_{\parallel}} u^*_{n,\vec{k}_{\parallel}}(\vec{r}_{\parallel},z) u_{n,\vec{k}_{\parallel}'}(\vec{r}_{\parallel},z) V(r_{\parallel},z) dv , \qquad (16)$$

where u is the periodic part of the Bloch function. The product $u^*_{n,\vec{k}_{\parallel}} u_{n,\vec{k}_{\parallel}'}$ can thus be expanded in a Fourier series,

$$u^*_{n,\vec{k}_{||}} u_{n,\vec{k}'_{||}} = \sum_{K_{||}} e^{i\vec{K}_{||}\cdot\vec{r}_{||}} C_{n,\vec{k}_{||},\vec{k}'_{||}}(K_{||},z) ,\tag{17}$$

leading to

$$\langle \varphi_{n,\vec{k}_{||}} | V | \varphi_{n,\vec{k}'_{||}} \rangle = \sum_{\vec{K}_{||}} \int d^2\vec{r}_{||} e^{i(\vec{k}'_{||}-\vec{k}_{||}+\vec{K}_{||})\cdot\vec{r}_{||}} \int dz\, C_{n,\vec{k}_{||},\vec{k}'_{||}}(\vec{K}_{||},z) V(\vec{r}_{||},z) .\tag{18}$$

As is usual in the 3D EMA (Ref. 14) we drop the $K_{||}\neq 0$ terms and approximate $C_{n,\vec{k}_{||},\vec{k}'_{||}}$ for values $\vec{k}_{||}$ and $\vec{k}'_{||}$ near the bottom $\vec{k}^0_{||}$ of the band by

$$C_{n,\vec{k}_{||},\vec{k}'_{||}} \cong C(z) ,\tag{19}$$

with $C(z)$ defined by

$$C(z) = \int |\varphi_{n,\vec{k}^0_{||}}(\vec{r}_{||},z)|^2 d^2 r_{||} .\tag{20}$$

If we note $U_n(\vec{r}_{||})$, the quantity

$$U_n(\vec{r}_{||}) = \int V(\vec{r}_{||},z) C(z) dz ,\tag{21}$$

and then the matrix element in (18) becomes the 2D Fourier transform $U_n(\vec{k}'_{||}-\vec{k}_{||})$ of $U_n(\vec{r}_{||})$. The basic equation (15) reduces to

$$[\epsilon_n(\vec{k}_{||})-E]a_{n,\vec{k}_{||}} + \sum_{\vec{k}'_{||}} U_n(\vec{k}'_{||}-\vec{k}_{||})a_{n,\vec{k}'_{||}} = 0 .\tag{22}$$

As in the 3D case this is the Fourier transform of the following differential equation:

$$[\epsilon_n(-i\vec{\nabla}_{||}) - E + U_n(\vec{r}_{||})]F_n(\vec{r}_{||}) = 0 ,\tag{23}$$

where $F_n(\vec{r}_{||})$ is the usual envelope function, i.e., the Fourier transform of $a_{n,k_{||}}$. If in (23), ϵ_n is expanded to second order we get the 2D effective mass equation,

$$\left[\epsilon_n(\vec{k}^0_{||}) - E - \frac{\hbar^2}{2m^*_{||}}\Delta_{||} + U_n(\vec{r}_{||})\right]F_n(\vec{r}_{||}) = 0 ,\tag{24}$$

in the isotropic case.

Thus we have just proved that the 2D EMA is applicable as long as impurity binding energies are smaller than the energy splitting between the subbands. If we take for the ratio of these two energies a limiting value of 0.25 then we find that our 2D treatment should be valid for

$$N \leq 10-15 .\tag{25}$$

The important point about the 2D EMA is that it contains an effective impurity potential $U_n(\vec{r}_{||})$ which is an average of $V(\vec{r}_{||},z)$ over z defined by (21). This can be performed if we know $\varphi_{n,\vec{k}^0_{||}}$, i.e., the solution of H_0 at the bottom of the nth subband.

V. APPLICATION OF THE 2D EMA TO THE TIGHT-BINDING s BAND

An application of this theory can be readily made to our test case of the tight-binding s band. In that case $\vec{k}^0_{||}=0$ for each subband whose Bloch function is

$$\varphi_{n,\vec{k}^0_{||}} = \frac{1}{\sqrt{N_{||}}} \sum_{i,l} C_{n,\vec{k}_{||}} e^{i\vec{k}_{||}\cdot\vec{R}_i} \varphi_{l,i} ,\tag{26}$$

where $\varphi_{l,i}$ is the atomic function of atom i in the lth plane (n is again the index of the subbands and varies from 1 to N).

Applying (21) and (20) with (26) and using approximations coherent with the tight-binding treatment one gets

$$U_n(\vec{r}_{||}) = \sum_l |C_{n,l}|^2 V(\vec{r}_{||},z_l) ,\tag{27}$$

where z_l refers to the position of the lth plane along the z axis. It is also well known that, in our simple case, the coefficients $|C_{n,l}|^2$ reduce to

$$|C_{n,l}|^2 = \frac{\sin^2[nl\pi/(N+1)]}{\sum_{l=1}^{N} \sin^2[nl\pi/(N+1)]}\tag{28}$$

for l varying from 1 to N.

We can compare our 2D EMA and effective potential $U_n(\vec{r}_{||})$ to what we have obtained directly in Sec. II for very narrow superlattices. We see that the equations to be solved are identical. A first very important conclusion is that our 2D treatment is valid for $N < 10-15$ and has the correct limiting behavior for very small N. It thus represents the desired solution to the problem when the 3D EMA does not apply.

In this tight-binding "test" case the effective potential $U_n(\vec{r}_{||})$ is defined as a finite series (27) in which the coefficients take the values given by (28). It is instructive to look at the intermediate situation with moderately large number of planes where the series can be approximated by an integral. In this case $U_n(\vec{r}_{||})$ becomes

$$U_n(\vec{r}_{||}) = \frac{\int_0^L \sin^2(n\pi z/L)V(\vec{r}_{||},z)dz}{\int_0^L \sin^2(n\pi z/L)dz} ,\tag{29}$$

where L is given by

$$L = Na .\tag{30}$$

The integral expression (29) is more tractable in practice than the series expansion of $U_n(\vec{r}_{||})$ and it is also more adapted to a comparison with the 3D EMA. We consider here only the lower subband and its 1s impurity state. We again choose for this state a variational envelope wave function of the form

$$F(\vec{r}_{||}) = Ae^{-\alpha|\vec{r}_{||}|} .\tag{31}$$

The corresponding binding energy $E_{1s}(\alpha)$ is given by

$$E_{1s}(\alpha) = \frac{\hbar^2\alpha^2}{2m_{||}} - \frac{16\alpha^2 e^2}{KL} \int_0^{L/2} \{(\pi/2)[H_1(2\alpha z) - N_1(2\alpha z)] - 1\}\cos^2(\pi z/L)dz \, , \tag{32}$$

which we minimize to obtain the optimum value.

The results of this calculation are plotted on Fig. 2 where they are compared to those of the discrete linear combination of atomic orbitals (LCAO) calculations. We can observe that there is significant difference only for very narrow superlattices (the maximum error for $N = 1$ represents only 13% of the binding energy, while for $N > 1$ it is practically negligible). The 2D EMA in its continuous version thus represents a quite accurate method for predicting the binding energies for moderately small number of planes ($N \leq 10-15$). As we have shown, for very narrow superlattices the 2D EMA can be reduced to its discrete version which gives essentially exact results.

VI. COMPARISON WITH THE 3D EMA MODEL OF BASTARD

We now compare our results with those of previous calculations and mainly the one by Bastard[8] based on the use of the 3D EMA. This work was mainly concerned by the lower impurity states derived from the lower subband. The Hamiltonian of the problem was taken to be

$$H = -\frac{\hbar^2}{2m^*}\Delta - \frac{e^2}{Kr} \tag{33}$$

within an infinite potential well of width L. To solve this problem for the ground $1s$ state, a trail function of the following form was used:

$$F_{1s} = A \sin(\pi z/L)e^{-\alpha r} \, , \tag{34}$$

which has 3D character in the exponential. From (33) and (34) a total energy E_{1s} was obtained under the form

$$E_{1s} = \epsilon_1 + \Delta E_{1s} \, , \tag{35}$$

where ϵ_1 is the bottom of the lower band for Hamiltonian (33) in the absence of the impurity potential, i.e.,

$$\epsilon_1 = \frac{\hbar^2}{2m^*}(\pi/L)^2 \, . \tag{36}$$

A first conclusion which emerges from this brief summary is that Bastard's model introduces two levels of approximation: one on ϵ_1 and another on E_{1s}. The first one corresponds to the fact that ϵ_1 given by (36) is certainly a very crude approximation to the exact bottom of the lower band for very narrow superlattices and this error is not easy to estimate in a general manner. If we now look at the binding energy we find that there the situation is much more encouraging. We have plotted in Fig. 3 the ΔE_{1s} of Bastard's 3D model and of our 2D model and find that they give practically the same answer for $N \leq 20$. After that the 3D result is lower, meaning that the 3D wave function is better for larger superlattices which is quite normal.

A first conclusion that emerges is that the binding energy of the $1s$ state predicted by the 3D EMA is extremely good. Thus its main deficiency is that it is not related to the exact bottom of the band but rather to an approximate value which can introduce easily errors of the order of the binding energy. In this regard the 2D EMA as derived here is superior since it gives a binding energy with respect to the exact bottom of the bands. Another strong interest of the 2D EMA treatment is that it applies equally well to each of the subbands, which is evidently not true of Bastard's model (where there is no systematic way of building wave functions for impurity states derived from excited subbands which are orthogonal to the lower states).
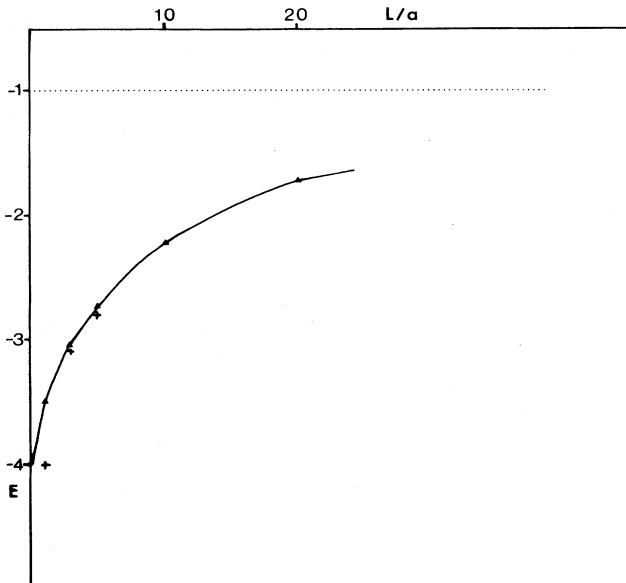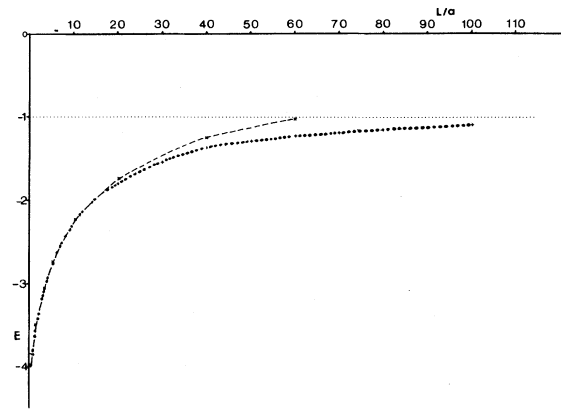

FIG. 2. Comparison of binding energies obtained by a continuous model (solid curve) and a discrete calculation (crosses). [Energy is reduced energy: $E/(m^*e^2/2K^2\hbar^2)$.]

FIG. 3. Binding energy of the lower state vs L, the width of the well (expressed in interatomic distance) obtained using 2D (dashed line) and 3D (dotted line) continuous models. [Energy is reduced energy: $E/(m^*e^2/2\hbar^2K^2)$.]
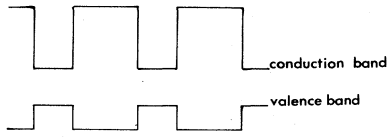
FIG. 4. Variations of the conduction and valence bands in a superlattice.

FIG. 5. Representation of an infinity of infinite wells of depth V_0, width a, and a periodicity of $L = a + b$.

This property is used in a forthcoming publication where it is applied to the study of the corresponding resonant states.[21]

VII. TUNNELING EFFECT

Up until now we have considered the case of an isolated infinite quantum well and thus neglected the tunneling effects between equivalent quantum wells. A simplified description of what happens in practice is given in Fig. 4. The most simple model accounting for that effect in the conduction band is provided by the periodic square-well structure of Fig. 5. Let us then discuss qualitatively what

happens.

The energy bands for one isolated square well are sums of $\hbar^2 |k_\parallel|^2/2m^*_\parallel$ plus the discrete levels resulting from quantification in the z direction. This gives rise to a step-like density of states, the spacing between the steps corresponding to the distance between the quantized levels. When considering the periodic structure of Fig. 5 these quantized states begin to interact and, as usual, broaden into bands. This broadening is unimportant when it is much smaller than the distance between steps in the density of states of one isolated quantum well.

We have studied the shift and broadening of the steps for different values of V_0, a, and b characterizing the periodic structure (Fig. 5). The allowed energies are given by the solutions of the following equation[24]:

$$\cos\frac{2\pi j}{N} = \cos\left[a\left[\frac{2mE}{\hbar^2}\right]^{1/2}\right]\cosh\left[b\left[\frac{2m}{\hbar^2}(V_0-E)\right]^{1/2}\right]$$

$$-\frac{2E-V_0}{2\sqrt{E(V_0-E)}}\sin\left[a\left[\frac{2mE}{\hbar^2}\right]^{1/2}\right]\sinh\left[b\left[\frac{2m}{\hbar^2}(V_0-E)]\right]^{1/2}\right]. \tag{37}$$

The allowed energies are drawn in Fig. 6 for varying values of the parameters. The product V_0a^2 controls the number of bands (i.e., the number of steps in the density of states) while b/a influences the broadening of the states into bands. It is seen that as soon as the potential well contains more than two states, then the broadening becomes negligible for $b/a > 1$. It is only when this condition is realized that our approximation of considering one isolated quantum well becomes valid. In Fig. 6 are also given the states corresponding to an infinite quantum well
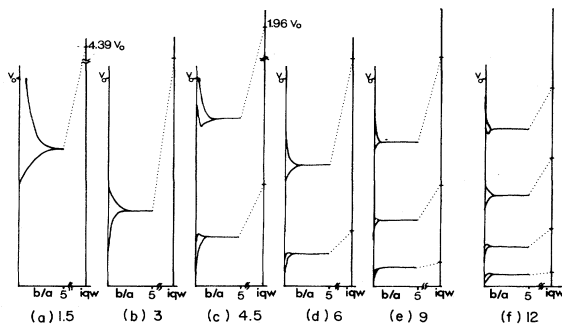
showing that this approximation introduces an appreciable error.

Finally we can apply Eq. (37) to the experimental situation observed by Dingle.[3] The characteristics of the potential wells and the corresponding bands are given in Fig. 7 where they are compared to the positions of the exciton lines. The fair agreement obtained shows that the periodic square-well potential model represents a good description of the actual system.

FIG. 6. Variations of allowed energies for the potential described by Fig. 5, as b/a varies, for different depths [in units of $(2mV_0a^2)^{1/2}/\hbar$] of wells. We have reported the levels of an isolated infinite quantum well (IQW).
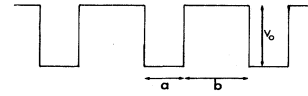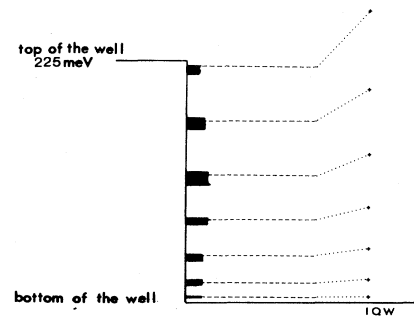

FIG. 7. Allowed energies calculated by (37) (dark areas) for the superlattice observed by Dingle (Fig. 12 of Ref. 3). We have reported the excitons observed by Dingle (dashed lines) and the levels of the isolated infinite quantum well (crosses). With the notation of Fig. 5 we have $V_0 = 225$ meV, $a = 316$ Å, $b = 250$ Å, and $m^* = 0.068$.

VIII. CONCLUSION

We have described in this work different approaches to the calculation of impurity states in superlattices based on the EMA. We have first performed an exact numerical test calculation for a single band and a narrow superlattice. We have then proposed a new 2D effective-mass scheme valid for moderate and small number of planes $N \leq 15$, but applicable to impurity states derived from all subbands. We have compared it to Bastard's 3D EMA, applicable to the lower states only, showing that both schemes lead to practically identical binding energies in the intermediate range $(3 \leq N \leq 15)$. Finally we have discussed the influence of tunneling between potential wells showing that it is not negligible in the experimental situations of interest.

A natural consequence of this work is the application of our 2D EMA to the calculation of the position and width of resonances associated with impurity states derived from excited subbands and thus falling into a continuum. This will be the subject of a planned forthcoming paper.

[1]L. Esaki and R. Tsu, IBM J. Res. Develop. 14, 61 (1970).

[2]For recent reviews, see G. S. Sai-Halasz, in *Physics of Semiconductors 1978,* edited by E. L. Wilson (IOP, London, 1979), p. 21, and various papers in Surf. Sci. 113 (1982).

[3]R. Dingle, in *Festkörperprobleme XV (Advances in Solid State Physics),* edited by M. J. Queisser (Pergamon, Vieweg, Braunschweig, 1975), p. 21.

[4]C. Weisbuch, R. C. Miller, R. Dingle, A. C. Gossard, and W. Wiegmann, Solid State Commun. 37, 219 (1981).

[5]R. C. Miller, D. A. Kleinman, W. T. Tsang, and A. C. Gossard, Phys. Rev. B 24, 1134 (1981).

[6]R. C. Miller, D. A. Kleinman, W. A. Nordland, Jr., and A. C. Gossard, Phys. Rev. B 22, 863 (1980).

[7]B. A. Vojak, N. Holonyak, Jr., W. D. Laidig, K. Hess, J. J. Coleman, and P. P. Dapkus, Solid State Commun. 35, 477 (1980).

[8]G. Bastard, Phys. Rev. B 24, 4714 (1981).

[9]L. Mailhiot, Y.-C. Chang, and T. C. McGill, Phys. Rev. B 26, 4449 (1982).

[10]L. J. Sham and M. Nakayama, Surf. Sci. 73, 272 (1978).

[11]M. Lannoo and J. Bourgoin, *Point Defects in Semiconductors—I,* Vol. 22 of *Springer Series of Solid State Sciences* (Springer, Berlin, 1981), Chap. II.

[12]J. C. Slater and G. F. Koster, Phys. Rev. 94, 1498 (1954).

[13]R. Haydock, in *Recursive Solution of the Schrödinger Equation,* Vol. 35 of *Solid State Physics,* edited by M. Ehrenreich, F. Seitz, and D. Turnbull (Academic, New York, 1980), p. 215.

[14]W. Kohn, in *Solid State Physics,* edited by F. Seitz and D. Turnbull (Academic, New York, 1957), Vol. 5, p. 258.

[15]J. Callaway, *Energy Band Theory* (Academic, New York, 1964).

[16]A. M. Stoneham, *Theory of Defects in Solids* (Clarendon, Oxford, 1975).

[17]S. T. Pantelides, Rev. Mod. Phys. 50, 797 (1978).

[18]F. Bassani, G. Iadonosi, and B. Preziosi, Rep. Progr. Phys. 37, 1099 (1974).

[19]B. Zaslow and M. E. Zandler, Ann. J. Phys. 35, 1118 (1967).

[20]L. Pauling and E. B. Wilson, *Introduction to Quantum Mechanics* (McGraw-Hill, New York, 1935), Chap. V.

[21]C. Priester, G. Allan, and M. Lannoo (unpublished).

[22]I. S. Gradshteyn and I. W. Ryzhik, *Table of Integrals Series and Products* (Academic, New York, 1965).

[23]C. Priester, M. Lannoo, and G. Allan (unpublished).

[24]D. Rapp, *Quantum Mechanics* (Holt, Rinehardt and Winston, New York, 1971), p. 120.